INTL JOURNAL OF ELECTRONICS AND TELECOMMUNICATIONS, 2015, VOL. 61, NO. 2, PP. 191–197
Manuscript received March 10, 2015; revised June 2015. DOI: 10.1515/eletel-2015-0025

Numerical Model of Directional Radiation Pattern Based on Primary Antenna Parameters

Piotr Jankowski-Mihułowicz, Wojciech Lichoń, and Mariusz Węglarski

***Abstract*—The new numerical model of directional radiation pattern, in which part of energy is emitted in side and back lobs, has been presented in this paper. The model input values are determined on the base of primary parameters that can be read from the datasheet of used antennas. The special software tool NmAntPat has been elaborated to carry out the described task. The elaborated model, program and output files can be easily implemented into an analysis of radio wave propagation phenomenon in any algorithms and numerical calculations. The comparison of the graphical plots that have been obtained on the base of measurements, producers' data specification notes and modelling results confirms the model correctness.**

***Keywords*—antenna, directional radiation pattern, modelling, radiocommunication**

I. INTRODUCTION

THE radiation pattern is the basic parameter of antennas. It allows designers to compare different solutions and assess their usefulness in wireless communication systems. The problem of modelling the radiation patterns for commercially available or own elaborated antennas is widely discussed in the branch literature. A few typical synthesis methods can be distinguished in this scope. The Schelkunoff polynomial method is used for modelling patterns of a linear antenna array [1], [2]. A complete description of the desired antenna pattern can be determine on the base of Fourier transforms (method known as beam shaping) [3]-[5]. The Woodward-Lawson procedure is often used to synthesis pattern of antenna arrays [6]-[8]. This is a popular method based on the Fourier-transform relationship between the field in a planar aperture and the far-field pattern. The binomial, Dolph-Tschebyscheff or Taylor methods are used for synthesising patterns with narrow main beams and low side lobes [9]-[11]. Also, methods of converting the real 3D radiation patterns (e.g. measured) into simple 2D models are elaborated in scientific investigations [12].

This work was supported in part by Polish National Centre for Research and Development (NCBR) under Grant No. PBS1/A3/3/2012. The work was developed by using equipment purchased in the Operational Program Development of Eastern Poland 2007-2013 of the Priority Axis I Modern Economics of Activity I.3 Supporting Innovation under Grant No. POPW.01.03.00-18-012/09-00 and the Program of Development of Podkarpacie Province of The European Regional Development Fund under Grant No. UDA-RPPK.01.03.00-18-003/10-00.

All the authors are with the Department of Electronic and Communications Systems, Rzeszów University of Technology, Pola 2, 35-959 Rzeszów, Poland (e-mail: pjanko@prz.edu.pl; w_lichon@prz.edu.pl; wmar@prz.edu.pl).

The mentioned methods lead to dependences that have to be solved by using advanced mathematical calculations. First of all, there is significant complexity with connecting the numerical calculations elaborated in this way and the basic parameters specified in antenna datasheets. It is the reason why only simple models of antenna patterns are developed in the branch literature, in the scope of practical implementation. They are usually dedicated to radio wave propagation calculations for a selected radio communication system [13], [14].

On the base of available subject literature, it can be stated that there is the need for developing simple tools by means of which it would be possible to generate a numerical representation of the radiation pattern for real antennas which work in a radio communication system. For this reason, the elaborated numerical model of directional radiation pattern, in which part of energy emitted in side lobs and back lobs is taken into consideration is discussed later in the article. The input values are determined on the base of primary parameters read from the antenna datasheets. On the base of model the useful software tools were worked out. The software can be used for both visualizing radiation pattern and also for generating file with discreet values of the pattern plot. The elaborated model, program and output file can be easily implemented into an analysis of radio wave propagation phenomenon in any algorithms and numerical calculations.

II. MODELLING ANTENNA PATTERNS

The radiation pattern reflects capability of energy radiation versus angles θ and ϕ of the spherical coordinate system [15] (Fig. 1). Also primary information that is used in activity characterization of a given radio communication system (such as: GSM, UMTS, LTE, WiFi, RFID and many others) can be derived on the base of this parameter.

The quantitative and qualitative estimation of radio communication system operation characteristics is essential in many contemporary research-development or design works. The knowledge about radiation patterns of transmitter (TX) and receiver (RX) antennas is always required for properly executing primary analytical and numerical calculations or advanced computer simulations of radio wave propagation (e.g. in the Radio Mobile of Roger Coudé freeware software [16], or the commercial – ICS Designer of ATDI [17]). These device's antennas and their radiation patterns have different geometrical configurations in diverse stationary or mobile radio communication systems (Fig. 1).

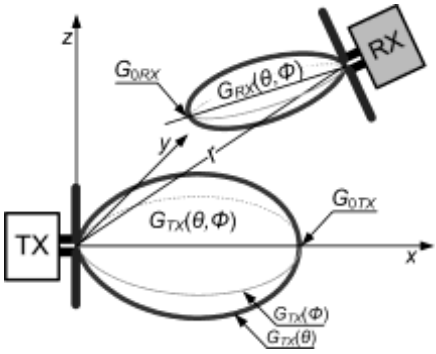

Fig. 1. Antennas in radio communication system

In many cases, the only source of information about antenna parameters is producers' technical specification notes. Usually they describe: radiation pattern diagrams in vertical $G(\theta)$ and horizontal plane $G(\phi)$, maximum value of the gain $G_0=G(\theta,\phi)|_{\max}$, half-power beam width *HPBW* of a main lobe, front-to-back ratio *FB*, side lobes level *SLL*, polarization (axial ratio), impedance parameters (standing wave ratio, return loss) and others. From a practical point of view, the crucial problem is the need of easy transformation from available plots of radiation patterns (e.g. presented in an antenna datasheet) to analytical dependences or discrete data required for numerical calculations of radio waves propagation. Authors stumbled across this problem in their research while the interrogation zone of an anti-collision radio frequency identification (RFID) system and also the maximum range of a base transceiver station ware determining. The process of entering specific points of the radiation pattern was extremely time-consuming on the stage of numerical model preparation. So, it was necessary to develop another means for accomplish this task.

The example of rough radiation pattern approximation can be illustrated on the base of simple 3GPP (3rd Generation Partnership Project) model [13]. The basic antenna parameters are used as input data for the calculations. The diagram of this pattern can be determined in the vertical plane by using the dependence [14]:

$$G(\theta)=\max\left(-12\cdot\left(\frac{\theta-TILT}{HPBW_\theta}\right)^2, SLL\right)\Bigg|_{-90^\circ\le\theta\le90^\circ} \quad (1)$$

whereas in the horizontal plane by:

$$G(\phi)=-\min\left(12\cdot\left(\frac{\phi}{HPBW_\phi}\right)^2, FB\right)+G_0\Bigg|_{-180^\circ\le\phi\le180^\circ} \quad (2)$$

where: $HPBW_\phi$, $HPBW_\theta$ mean half power beam width in adequately vertical and horizontal planes whereas *TILT* denotes tilting of the main beam.

The visualization of the dependences (1) and (2) is presented in the Fig. 2 for hypothetical data of a given antenna solution considered in practical tests ($HPBW_\phi$ =60°, $HPBW_\theta$=15°, G_0=6 dBi, *FB*=22 dB, *SLL*=-30 dB, *TILT*=30°).

Only the main lobe of antenna radiation pattern can be usually approximated by using such a model. There is no possibility to take into consideration exact characteristics of scattering for emitted energy in side and back lobs. It limits model usefulness to simple schemes of radio wave propagation such as in [18].

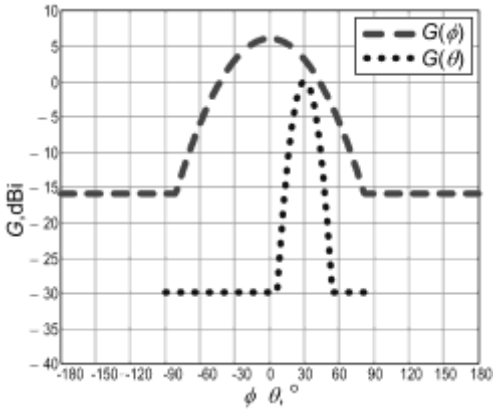

Fig. 2. Example of antenna patterns for a simple model based on 3GPP

III. Numerical Model

The elaboration of numerical model of directional radiation pattern has been the main goal of the work. The utility program called *NmAntPat* has been elaborated on the base of this model. It may be used to determine all points of considered plots. The investigations were dedicated to any radio communication system. The essence of the method consists in the power gain diagram *G* calculation conducted in vertical (θ) or horizontal (ϕ) plane. It is represented by the function *NmAntPat*:

$$G(\theta,\phi)=NmAntPat\begin{pmatrix}G_0, HPBW, HPBW_{back},\\ FS, FB, FB_{rest}, n_{side}, n_{back},\\ ANG, TILT\end{pmatrix} \quad (3)$$

Arguments of the function *NmAntPat* are basic parameters of the modelled antenna: G_0 – maximum value of the gain (dBi), *HPBW* – half-power beam width of the main lobe (°), $HPBW_{back}$ – half-power beam width of the main back lobe (°), *FS* – front-to-side ratio (dB), *FB* – front-to-back ratio (dB), FB_{rest} – front-to-back ratio of the back lobes (dB), n_{side} – number of the side lobes (equal distribution in the range from 0° to 180°), n_{back} – number of the back lobes (equal distribution in the range from 180° to 360°), *ANG* – variable θ in vertical or ϕ in horizontal plane (from 0° to 360°), *TILT* – tilting of the pattern (°). The model parameters are illustrated in Fig. 3. The model synthesis is discussed only for the angle θ as an example. The calculations are similar for orthogonal planes.

The normalized power pattern in the plane of angle θ can be shown in a linear $P_n(\theta)$ or logarithmic scale $P_{n.dB}(\theta)$ where:

$$P_{n.dB}(\theta)=10\cdot\log\left(P_n(\theta)\right) \quad (4)$$

The pattern is modelled as a superposition of the lobs. The main and side lobs are estimated at an angle in the range of [0°,180°), whereas the back lobes – in the range of [180°,360°). The main lobe of directional pattern is determined from the expression:

$$P_{n.main}(\theta)=\left(\sqrt{\sin(\theta)}\right)^N \quad (5)$$

where *N* means a variable, that is used for estimating a width of the modelled lobe (Fig. 4).

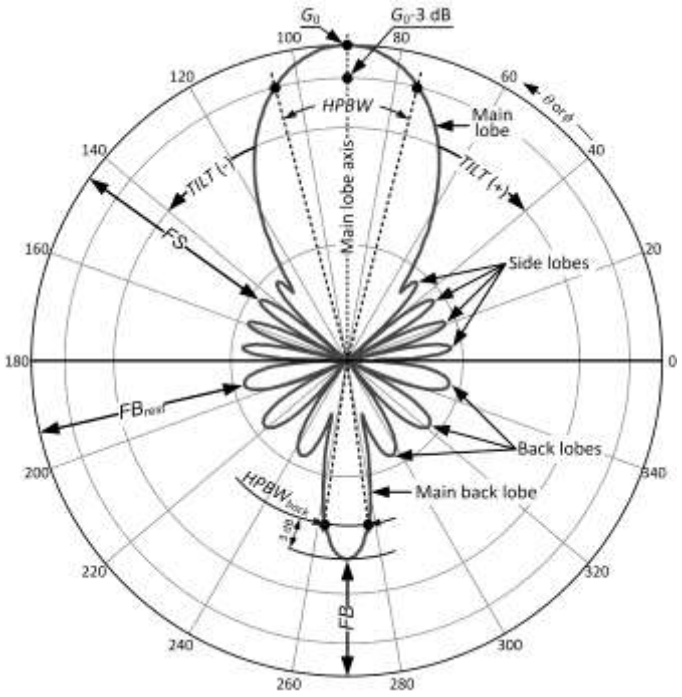

Fig. 3. Modelled radiation pattern

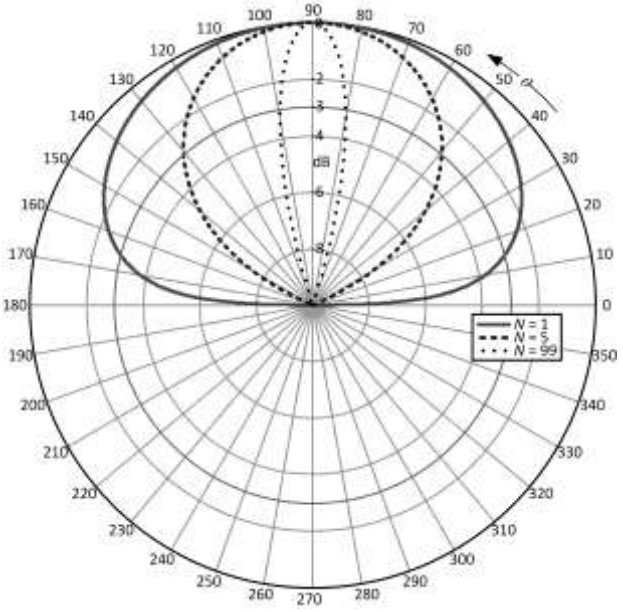

Fig. 4. The influence of variable *N* on a width of the main lobe

The primary parameters of the real antenna (measured or gathered from datasheets) have been taken into consideration as the arguments of function *NmAntPat*, instead of hypothetical data usually assumed in numerical models. Therefore, it was necessary to elaborate own algorithm for determining *N* coefficient. The algorithm was dedicated for a given half power width *HPBW* of the main lobe (Fig. 5).

Calculations with the accuracy (0.01) assumed for *N* variable provide results with acceptable rate and precision. It leads to accurate approximation of the radiation pattern for a real antenna.

The main back lobe is simulated in the similar manner. The level of the back lobe may be adjusted by using variable q_{back}. The modification of the expression (5) is necessary because of less energy in considered lobe:

$$P_{n.back}(\theta) = \frac{\left(\sqrt{\sin(-\theta)}\right)^{N_{back}}}{q_{back}} \tag{6}$$

where N_{back} means the variable that is used in the procedure of searching the proper width of modelled back lobe on the base of half power beam width $HPBW_{back}$.

The q_{back} model parameter is obtained directly on the base of front-to-back ratio (dB):

$$q_{back} = 10^{\frac{FB}{10}} \tag{7}$$

The impact of q_{back} value change on the level of main back lobe is presented on directional pattern in Fig. 6.

The side lobes $P_{n.side}(\theta)$ and the rest of back lobes $P_{back.rest}(\theta)$ are calculated by analogy to previously described rules, wherein:

$$P_{n.side}(\theta) = \frac{\left|\sin(n_{side}\theta)\right|}{q_{side}} \tag{8}$$

$$P_{n.back.rest}(\theta) = \frac{\left|\sin(n_{back}\theta)\right|}{q_{back.rest}} \tag{9}$$

where q_{side} and $q_{back.rest}$ model parameters result from front-to-side ratio (dB) and front-to-back ratio of the back lobes (dB) correspondingly:

$$q_{side} = 10^{\frac{FS}{10}} \tag{10}$$

$$q_{back.rest} = 10^{\frac{FB_{rest}}{10}} \tag{11}$$

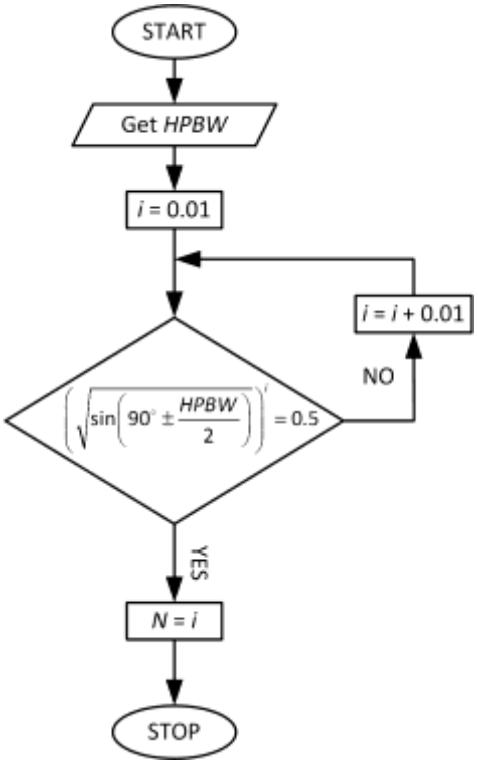

Fig. 5. The algorithm of *N* variable determination on the base of half power beam width

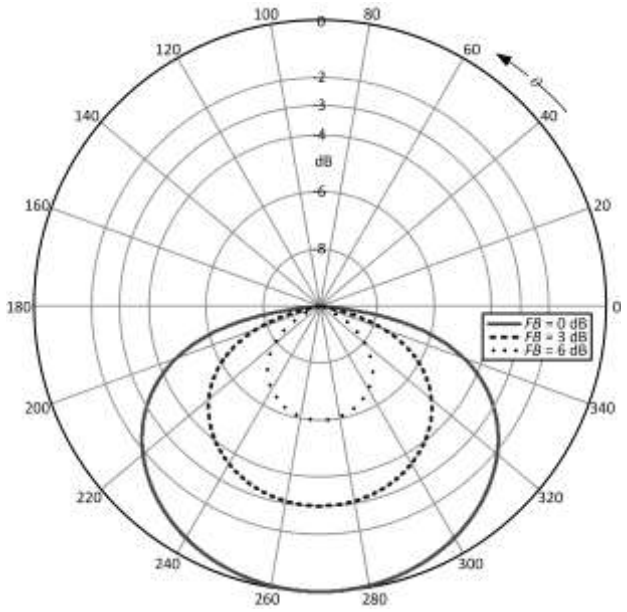

Fig. 6. The impact of *FB* variable on the main back lobe ($HPBW_{back}$=constant)

The number of the side lobes (n_{side}) and number of the back lobes (n_{back}) are included in dependences (8) and (9). Such a conception allows for accurately mapping of energy radiated in the side lobes. It significantly increases the approximation accuracy in the process of determining the real antenna radiation pattern.

The *NmAntPat* program implemented in Mathcad environment not only visualizes the radiation patterns but also generates files for subsequent data processing (Fig. 7). A user may select any format that is typical for data of this kind. It is useful during further analysis of radio wave propagation phenomena. So, it can be utilized in any user algorithm, freeware or commercial platform. The file has been utilized during preparation of graph visualisation in graphing and data analysis software package Origin.

The main software procedure *NmAntPat* (Fig. 8) comprises the derived dependences (3)-(11). An additional procedure is used for calculating and visualising values of every lobe levels (Fig. 7). It simplifies the approximation of modelled radiation pattern.

IV. Experiment

The problem of radiation pattern synthesis is presented on the base of practical case. A real antenna of read/write device (Feig ID ISC.ANTU250/250 in EU version [19]) working in the UHF band of radio-frequency identification RFID system has been selected. It should be emphasised that the precision in model synthesis is especially crucial in the selected range of frequency. Since, both data and energy are conveyed between transmitter and receiver (RWD and transponders in which chips are powered by electromagnetic field generated by RWD's antenna) small discrepancies can lead to lack of identification. The interrogation zone (IZ) is the most useful parameter on the stage of designing the RFID systems [20], [21] and it is used as the factor of proper synthesis process.

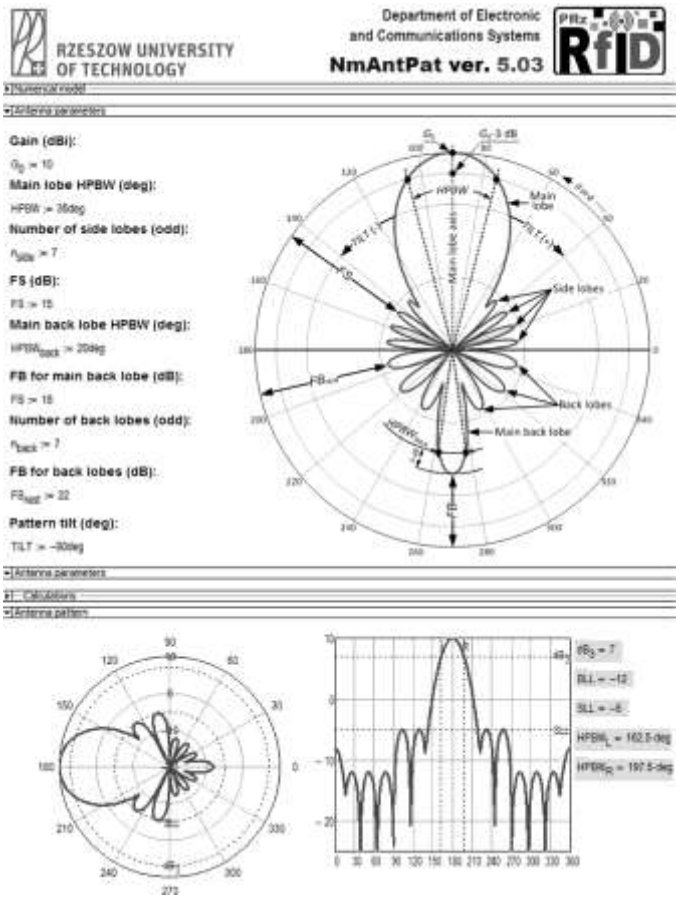

Fig. 7. *NmAntPat* program

The critical step is to select adequate input data. Firstly, it should be done on the base of producer datasheets [19]. Unfortunately, these technical specifications are often incomplete or not precise. So, same parameters have to be measured by designers. In the prescribed experiment, the missing data have been determined in the laboratory stand of RFID system that had been especially prepared for this aim at the Department of Electronic and Communications Systems at Rzeszów University of Technology (Fig. 9).

The measurements were done in the TDK (18 GHz) anechoic chamber with using the MI Technologies antenna system: Sunol Sciences elevation over azimuth positioner ELAZ75 and system controller SC110V, vector network analyser Agilent PNA-X N5242A, MI 3003 workstation with MI Arena software, tuned dipole antenna set A.H. Systems TDS-535 (25-1000 MHz) and others equipment (INNCO Systems, R&S).

The comprising chart of directional radiation patterns is presented in Fig. 10. The first diagram has been gathered from producer specification note, the second one – on the base of measured data. It can be noticed that the convergence of characteristics is high for the main lobe and satisfactory for the rest of directions. The minor discrepancies in back lobes may arise from the lack of precise information about the frequency used in a test procedure described in datasheets. The frequency of the measuring procedure has been established on 868 MHz in the carried out experiment.

$$\text{NmAntPat}(G_0, HPBW, HPBW_{back}, FS, FB, FB_{rest}, n_{side}, n_{back}, ANG, TILT) :=$$

for $i \in 0,1,0.2..500$

$N \leftarrow i \text{ if } \left(\sqrt{\sin\left(90\text{deg} - \frac{HPBW}{2}\right)}\right)^i \geq 0.5$

for $i \in 0,1,0.2..500$

$N_{back} \leftarrow i \text{ if } \left(\sqrt{\sin\left(90\text{deg} - \frac{HPBW_{back}}{2}\right)}\right)^i \geq 0.5$

$q_{side} \leftarrow 10^{\frac{FS}{10}}$

$q_{back} \leftarrow 10^{\frac{FB}{10}}$

$q_{back.rest} \leftarrow 10^{\frac{FB_{rest}}{10}}$

$G_{cal} \leftarrow 10^{\frac{G_0}{10}}$

$ANG \leftarrow ANG + TILT$

if $ANG \leftarrow ANG - 360\text{deg}$ if $ANG + TILT \geq 360\text{deg}$

$TILT \leq ANG + TILT \leq TILT + 180\text{deg}$

$a \leftarrow \left(\sqrt{\sin(ANG)}\right)^N$ if $\left(\sqrt{\sin(ANG)}\right)^N > \frac{\left|\sin\left[n_{side}(ANG)\right]\right|}{q_{side}}$

$a \leftarrow \frac{\left|\sin\left[n_{side}(ANG)\right]\right|}{q_{side}}$ if $\left(\sqrt{\sin(ANG)}\right)^N < \frac{\left|\sin\left[n_{side}(ANG)\right]\right|}{q_{side}}$

otherwise

$a \leftarrow \frac{\left[\sqrt{\sin(-ANG)}\right]^{N_{back}}}{q_{back}}$ if $a \leftarrow \frac{\left(\sqrt{\sin(-ANG)}\right)^{N_{back}}}{q_{back}} > \frac{\left|\sin\left[n_{back}(ANG)\right]\right|}{q_{back.rest}}$

$a \leftarrow \frac{\left|\sin\left[n_{back}(ANG)\right]\right|}{q_{back.rest}}$ if $\frac{\left(\sqrt{\sin(-ANG)}\right)^{N_{back}}}{q_{back}} < \frac{\left|\sin\left[n_{back}(ANG)\right]\right|}{q_{back.rest}}$

return $G_{cal} \cdot a$

Fig. 8. *NmAntPat* procedure

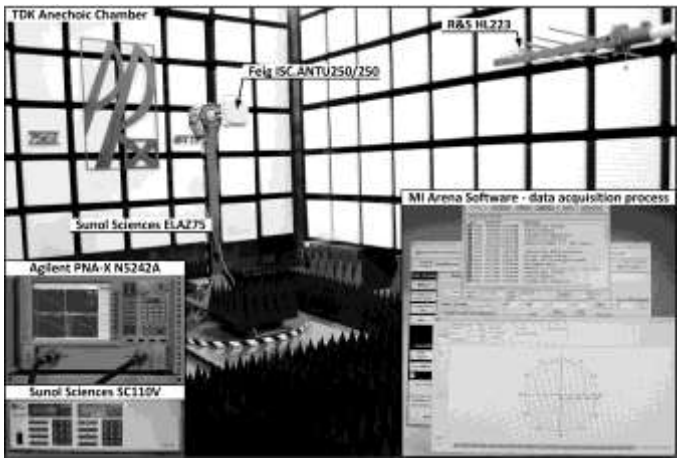

Fig. 9. Measurement test stand

TABLE I
COMPARISON OF MAIN PARAMETERS OF GATHERED AND MEASURED RADIATION PATTERN FOR INVESTIGATED ANTENNA

Parameter	Datasheet	Measurement
G_0	7.4 dBi	7.6 dBi
$HPBW$	60°	58°
n_{side}	2	2
FS	12 dB	18 dB
$HPBW_{back}$	45°	45°
FB	14.7 dB	11.6 dB
n_{back}	3	3
FB_{rest}	23.7 dB	16.3 dB

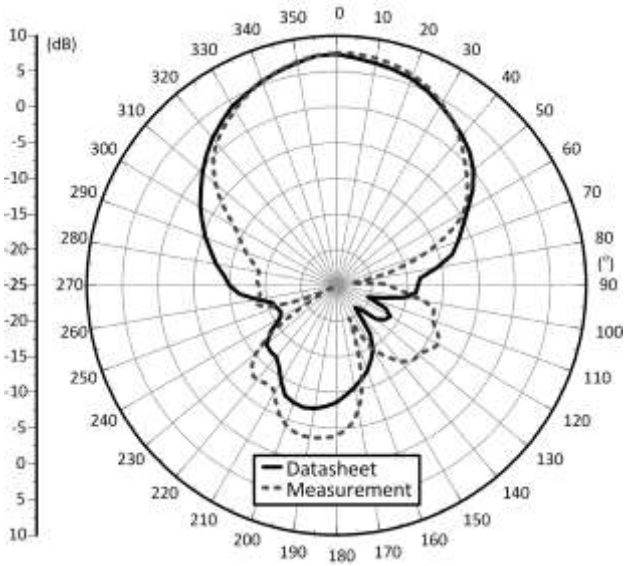

Fig. 10. Diagram comparison of gathered and measured radiation pattern for investigated antenna

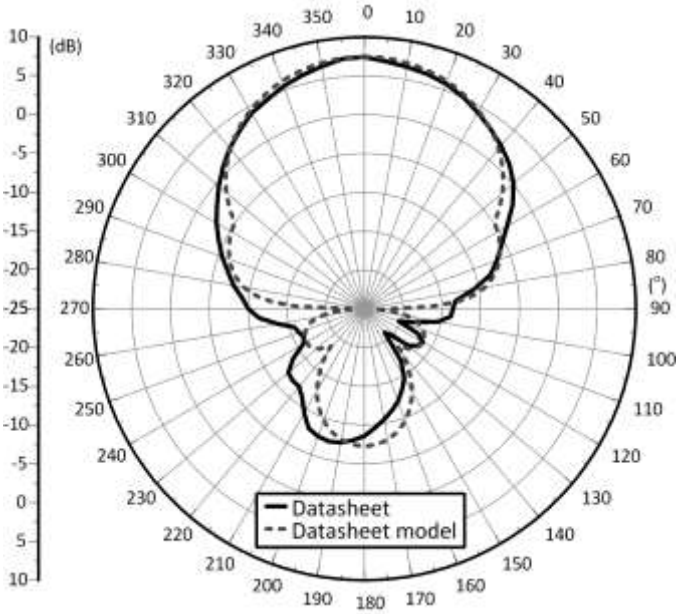

Fig. 11. Charts of radiation pattern determined on the base of producer specification notes

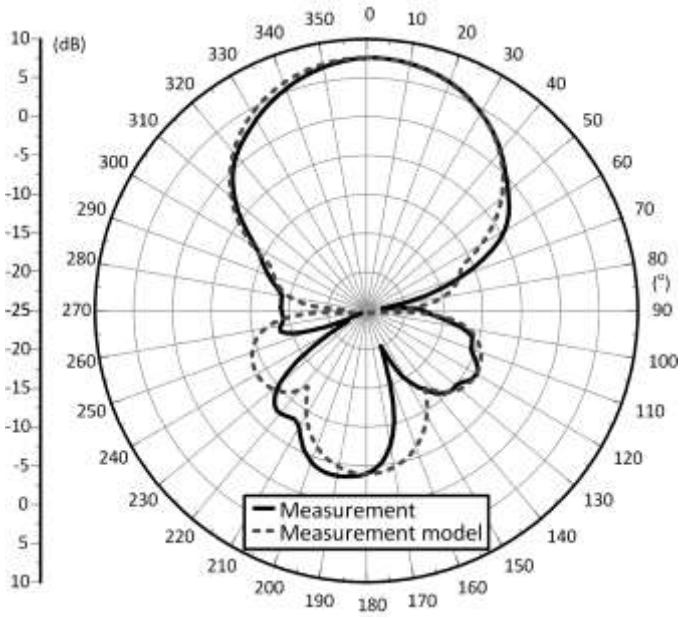

Fig. 12. Charts of radiation pattern determined on the base of research measurements

The comparison of main parameters of radiation pattern is presented in Table I. These values are used as input data for the numerical model of synthesis process applied to antenna under test. The elaborated program *NmAntPat* has been utilized in the experiment. So, the involved model has been evaluated on the base of both measured and gathered values of parameters. Its visualization is presented separately in Fig. 11 and Fig. 12 correspondingly.

The comparison of main parameters of radiation pattern is presented in Table I. These values are used as input data for the numerical model of synthesis process applied to antenna under test. The elaborated program *NmAntPat* has been utilized in the experiment. So, the involved model has been evaluated on the base of both measured and gathered values of parameters. Its visualization is presented separately in Fig. 11 and Fig. 12 correspondingly.

The both presented cases give satisfactory results and convergence of determined radiation pattern. It shows the practical utility of the developed model and software tools. The preparatory studies revealed vagueness of data specification notes published by manufacturers for their products. The lack of important parameter values makes a radio communication system synthesis (e.g. interrogation zone in RFID system) very difficult and shared information is not sufficient to reproduce the characteristics of the antenna. But, an accurate analysis of the specified radiation pattern can lead to determine missing input data for proper implementation of antennas in real environment.

V. Conclusion

The developed algorithm and software tools greatly facilitate the efficient use of radiation pattern for designing any kind of radio communication systems. The values of parameters calculated by using elaborated method can be quickly adopted in sophisticated research on problems connected with synthesising radio propagation systems. The output files can be easily visualised in graphing and data analysis software or can be implemented into any analysis of radio wave propagation phenomenon in any algorithms and numerical calculation.

The comparison of radiation patterns that have been obtained on the base of measurements, producers' data specification notes and modelling results confirms the model correctness. From a practical point of view, the elaborated model has been presented on the example of real antenna applied in read/write devices working in UHF band of RFID system. Authors encountered the necessity to solve presented problems while they were synthesizing the interrogation zone in RFID systems. The process of entering specific points of the radiation pattern was extremely time-consuming, so the possibility to determine important parameters by computer-aided analysis was very useful.

References

[1] B. Lindmark, B. "Analysis of pattern null-fill in linear arrays," in Proc. of the 7th European Conference Antennas and Propagation (EuCAP), Gothenburg (Sweden), 2013, p. 1457–1461.

[2] S. Choudhari, K. P. Ray and S. Kulkarni, "Design and development of 4 element linear microstrip patch antenna array with null steering by phase control," in Proc. of the International Conference Sustainable Energy and Intelligent Systems (SEISCON), Chennai (India), DOI: 10.1049/cp.2011.0441, 2011, p. 645–649.

[3] J. Adam, L. Klinkenbusch, H. Mextorf and R. H. Knochel, "Numerical multipole analysis of ultrawideband antennas," IEEE Transactions on Antennas and Propagation, DOI: 10.1109/TAP.2010.2078448, vol. 58, no. 12, p. 3847–3855, 2010.

[4] J. Gomez-Tornero, A. Martinez-Ros and R. Verdu-Monedero, "FFT synthesis of radiation patterns with wide nulls using tapered leaky-wave antennas," IEEE Antennas and Wireless Propagation Letters, DOI: 10.1109/LAWP.2010.2051314, vol. 9, pp. 518–521, 2010.

[5] K. Yang, Z. Zhao and Q. H. Liu, "Fast pencil beam pattern synthesis of large unequally spaced antenna arrays," IEEE Transactions on Antennas and Propagation, DOI: 10.1109/TAP.2012.2220319, vol. 61, no. 2, pp. 627–634, 2013.

[6] F. Ares-Pena and J. A. Rodriguez-Gonzalez, "Antenna array pattern synthesis for space communication applications," In Proc. of the IEEE Antennas and Propagation Society International Symposium (APS/URSI), Toronto (Canada), DOI: 10.1109/APS.2010.5561769, 2010, pp. 1–4.

[7] M. D. Migliore, "MIMO antennas explained using the Woodward-Lawson synthesis method," IEEE Antennas and Propagation Magazine, DOI: 10.1109/MAP.2007.4395337, vol. 49, no. 5, pp. 175–182, 2007.

[8] J. -S. Jang, N. -H. Kang, Y. W. Koo and J. -K. Ha, "Planar array antenna design with beam shaping for ETCS-RSE," In Proc. of the Asia-Pacific Microwave Conference Proceedings (APMC), Seoul (Korea), DOI: 10.1109/APMC.2013.6695064, 2013, pp. 1185–1187.

[9] N. H. Noordin, A. T. Erdogan, T. Arslan and B. Flynn, "Low side lobe level synthesis for linear faceted adaptive antenna arrays," In Proc. of the Loughborough Antennas and Propagation Conference (LAPC), Loughborough (UK), DOI: 10.1109/LAPC.2012.6402989, 2012, pp. 1–5.

[10] A. Falahati, M. Naghshvarian Jahromi and R. M. Edwards, "Wideband fan-beam low-sidelobe array antenna using grounded reflector for DECT, 3G, and ultra-wideband wireless applications," IEEE Transactions on Antennas and Propagation, DOI: 10.1109/TAP.2012.2226224, vol. 61, no. 2, pp. 700– 706, 2013.

[11] J. A. Rodriguez-Gonzalez, J. Fondevila-Gomez and F. Ares, "Rapid method for obtaining footprint patterns for very large antenna arrays," Electronic Letters, DOI: 10.1049/el:20082918, vol. 44, no. 4, pp. 264–265, 2008.

[12] H.Kanj, P. Lusina, S. M. Ali and F. Kohandani, "A 3D-to-2D transform algorithm for imcorporating 3D antenna radiation pattern in SCM," IEEE Antennas and Wireless Propagation Letters, DOI: 10.1109/LAWP.2009.2026301, vol. 8, pp. 815–818, 2009.

[13] ETSI, Universal Mobile Telecommunications System (UMTS); Spatial channel model for Multiple Input Multiple Output (MIMO) simulations. 3GPP TR 25.996, ver. 11.0.0, Release 11, 2012.

[14] F. Gunnarsson et al., "Downtilted base station antennas – a simulation model proposal and impact on HSPA and LTE performance," In Proc. of the 68th IEEE Vehicular Technology Conference (VTC Fall), Calgary (Canada), DOI: 10.1109/VETECF.2008.49, 2008, pp. 1–5.
[15] C. Balanis, Antenna Theory – Analisys and Design. 3rd Ed. Wiley, 2005.
[16] B. J. Henderson, "Radio mobile – radio propagation and radio coverage computer simulation program," Program operating guide, ver. 4.0, Calgary (Canada), 2013.
[17] S. Nedhif, "Guidelines for a LTE Network Design and Optimisation with ICS Designer," datasheet, ver. 1.3, ATDI, 2014.
[18] ETSI, "3rd Generation Partnership Project; Technical Specification Group Radio Access Network; Physical layer aspects for evolved Universal Terrestrial Radio Access (UTRA)," 3GPP TR 25.814, ver. 7.1.0, Release 7, 2006.
[19] FEIG, "ID ISC.ANTU250/250, Type EU and FCC, UHF Long Range Antenna," datasheet, document M40900-3de-ID-B, 2006.
[20] P. Jankowski-Mihułowicz and D. Kawalec, "The synthesis of a UHF RWD antenna as a step for determining the interrogation zone in RFID systems," Telecommunication Review + Telecommunication News, vol. 8–9, pp. 1077–1084, 2013.
[21] P. Jankowski-Mihułowicz, W. Kalita, M. Skoczylas and M. Węglarski, "Modelling and design of HF RFID passive transponders with additional energy harvester," International Journal of Antennas and Propagation, DOI: 10.1155/2013/242840, ID.242840, pp. 1–10, 2013.